

# The potential role of stratospheric ozone in the stratosphere-ionosphere coupling during stratospheric warmings

L. P. Goncharenko,<sup>1</sup> A. J. Coster,<sup>1</sup> R. A. Plumb,<sup>2</sup> and D. I. V. Domeisen<sup>2</sup>

Received 7 February 2012; revised 9 March 2012; accepted 9 March 2012; published 18 April 2012.

[1] The recent discovery of large ionospheric disturbances associated with sudden stratospheric warmings (SSW) has challenged the current understanding of mechanisms coupling the stratosphere and ionosphere. Non-linear interaction of planetary waves and tides has been invoked as a primary mechanism for such coupling. Here we show that planetary waves may play a more complex role than previously thought. Planetary wave forcing induces a global circulation that leads to the build-up of ozone density in the tropics at 30–50 km altitude, the primary region responsible for the generation of the migrating semidiurnal tide. The increase in the ozone density reaches 25% and lasts for ~35 days following the SSW, long after the collapse of the planetary waves. Ozone enhancements are not only associated with SSW but are also observed after other amplifications in planetary waves. In addition, the longitudinal distribution of the ozone becomes strongly asymmetric, potentially leading to the generation of non-migrating semidiurnal tides. We report a persistent increase in the variability of ionospheric total electron content that coincides with the increase in stratospheric ozone and we suggest that the ozone fluctuations affect the ionosphere through the modified tidal forcing. **Citation:** Goncharenko, L. P., A. J. Coster, R. A. Plumb, and D. I. V. Domeisen (2012), The potential role of stratospheric ozone in the stratosphere-ionosphere coupling during stratospheric warmings, *Geophys. Res. Lett.*, 39, L08101, doi:10.1029/2012GL051261.

## 1. Introduction

[2] Stratospheric sudden warming (SSW) events have recently received significant attention as primary examples of the strong vertical coupling between the different atmospheric levels. Series of recent results have presented a strong evidence of large variations in the upper atmosphere (above 100 km) during SSW events. Alternating layers of warming in the lower thermosphere (~120–140 km) and cooling in the ionosphere above ~150 km were reported at the middle latitudes by *Goncharenko and Zhang* [2008]. Surprisingly large variations in vertical ion drifts were observed in the low-latitude ionosphere [*Chau et al.*, 2009]. Disturbances in the ion drift variations at the magnetic equator drive profound changes in the low-latitude electron density and significantly contribute to the variability of the equatorial ionization anomaly [*Goncharenko et al.*, 2010a,

2010b; *Pancheva and Mukhtarov*, 2011; *Liu et al.*, 2011]. An important characteristic of ionospheric disturbances related to the SSW is their apparent tidal nature: increase in the vertical ion drift and total electron content was followed by a decrease 6 hours later, leading to the hypothesis about amplified semidiurnal tides in the low-latitude lower thermosphere during SSW events.

[3] As SSW events are driven by strong enhancements in the quasi-stationary planetary wave activity, it has been suggested that the coupling between the stratosphere and the ionosphere occurs through the non-linear interaction of planetary waves and tides. Both numerical simulations and observations support this suggestion. Analysis of GPS TEC (Total Electron Content) data has found an increase in the amplitudes of both migrating and non-migrating semidiurnal tides during SSW events [*Pedatella and Forbes*, 2010]. Numerical simulations have demonstrated amplifications of tidal modes in the mesosphere-lower thermosphere region [*Liu et al.*, 2010; *Fuller-Rowell et al.*, 2011]. Both migrating and non-migrating tides can be affected, resulting in a complex spatio-temporal pattern in the lower thermosphere. The TIMEGCM model indicates an increase in the 24-h tide and 12-h tides [*Liu et al.*, 2010], while the WAM model shows a decrease in the 12-h wave and a pronounced increase in the amplitude of an 8-h tide [*Fuller-Rowell et al.*, 2011]. Simulations by *Liu et al.* [2010] show the maximum increase in 12-h tides 1 day after the peak in planetary wave activity. However, experimental observations demonstrate that the maximum ionospheric disturbances are observed several days later [*Chau et al.*, 2009; *Goncharenko et al.*, 2010a, 2010b; *Liu et al.*, 2011], i.e., when planetary wave activity has already decreased. Important discrepancies between the model simulations and observations seem to indicate that, in addition to the non-linear interaction between planetary waves and tides, other mechanisms might be involved.

[4] The semidiurnal migrating tide is generated by the interaction of solar radiation with stratospheric ozone, which maximizes around 10°S in January [*Hagan et al.*, 1999]. The ozone heating peaks at ~45 km altitude with an approximate Gaussian distribution above and below this height, and the most important contributions are coming from between 30–60 km [*Forbes and Garrett*, 1978]. To gain further insight into the coupling processes between the stratosphere and the ionosphere, we use stratospheric data from the European Center for Medium Range Weather Forecast (ECMWF) and ionospheric data from GPS TEC for a case study of winter 2008/09.

## 2. Data

[5] For a description of variations in stratospheric parameters we use ERA-Interim data, which is the latest global

<sup>1</sup>Haystack Observatory, Massachusetts Institute of Technology, Westford, Massachusetts, USA.

<sup>2</sup>Department of Earth, Atmospheric and Planetary Sciences, Massachusetts Institute of Technology, Cambridge, Massachusetts, USA.

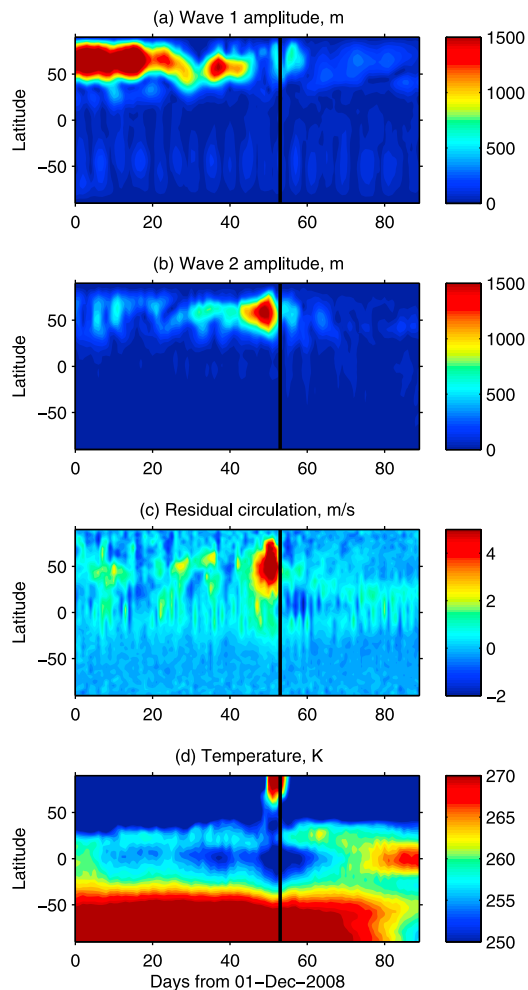


**Figure 1.** Development of planetary wave activity for (a) wave 1 and (b) wave 2, (c) residual mean meridional circulation  $v^*$  [e.g., Andrews *et al.*, 1987], and (d) temperature in Dec 2008–Feb 2009. All figures at 2 hPa. The increase in planetary wave activity at high latitudes induces an enhanced northward residual circulation between 20°S–80°N and a cooling in the tropics. Vertical lines indicate Jan 23, 2009, the peak of stratospheric temperature at 90°N and 10 hPa during the major SSW.

atmospheric reanalysis produced by the ECMWF [Dee *et al.*, 2011]. The data is provided globally with  $1.5 \times 1.5$  degree horizontal resolution and 6 hours temporal resolution. The top level of the data set is 1 hPa ( $\sim 48$  km).

[6] For this study we also use maps of global total electron content (TEC) that were obtained by MIT Haystack Observatory [Rideout and Coster, 2006] from over 2000 worldwide GPS receivers. The TEC estimates are produced in  $1^\circ \times 1^\circ$  bins of latitude/longitude with 5 minutes temporal resolution and distributed over those locations where data is available. More details on GPS TEC analysis are given by Goncharenko *et al.* [2010b].

### 3. Results

[7] We focus on the analysis of stratospheric data in the upper stratosphere, as both the planetary waves as well as the migrating semidiurnal tide are produced below that level.

Planetary-scale disturbances are almost always present during Northern Hemisphere winter. Figure 1 presents the evolution of planetary wave amplitude computed from geopotential height for the winter 2008/09 at the 2 hPa level. The two main features of interest here are the temporal and spatial development in planetary wave activity. Planetary wave 1 (Figure 1a) is strongly amplified in early December (days 1–20) and in early January (days 34–40), with only moderate enhancement during the SSW event. Planetary wave 2 amplitude (Figure 1b) reaches a maximum on January 17, 2009, and decreases sharply as the SSW develops. Anomalous low stratospheric planetary wave activity during the mature stage of a SSW is a well-established behavior [Limpasuvan *et al.*, 2004], as planetary waves generated in the troposphere cease to propagate into the stratosphere due to the change in zonal mean flow. Another important feature is that high planetary wave activity is limited to the latitude range of 40–80°N, and is much weaker at lower latitudes, where the semidiurnal migrating tide is generated.

[8] Amplifications of high-latitude planetary waves are accompanied by significant anomalies in the residual mean circulation (Figure 1c). At the 2 hPa pressure level, this circulation exhibits an enhanced northward flow between 20°S and 80°N during the build-up to the SSW event. In addition, stratospheric cooling on the order of 5–15 K is observed in the tropics (Figure 1d).

[9] Disturbances to the stratospheric circulation can have profound effects on the distribution of stratospheric ozone, which is a primary source for the generation of the migrating semidiurnal tide. Analysis of zonal mean ozone mixing ratio at 2 hPa ( $\sim 43.5$  km), close to the altitude of peak tidal heating, indicates that during the periods of tropical cooling the low-latitude ozone density has increased (Figure 2a). This increase in the ozone density is most pronounced around the peak of SSW, but is also observed during the periods of tropical cooling (days  $\sim 10$ –20 and  $\sim 30$ –40) that follow amplifications of planetary wave 1 or 2 (Figure 1). An increase in the ozone density at 2 hPa is observed over a large range of latitudes and extends to  $\sim 30^\circ$ N during the SSW. Figure 2b shows ozone changes with time and pressure level, presented as percentage difference with respect to the mean ozone density on Dec 1–10, 2008 at 25°S–5°N. Perturbations in the ozone density are positive in the upper stratosphere (above 10 hPa,  $\sim 30$  km), with peaks reaching 6%, 13%, and 25% between 40–45 km (2–3 hPa), and are coincident with the disturbances in the residual circulation driven by the planetary waves. In the lower stratosphere, below 10 hPa (30 km), ozone perturbations are negative, have magnitudes of the order of 5–10%, and are superimposed on a negative seasonal trend.

[10] Fritz and Soules [1970] have documented the cooling in the tropical stratosphere during SSW events. Randel [1993] reported global variations in zonal mean ozone during stratospheric warmings based on eight years of SBUV data. Changes in stratospheric parameters in winter 2008/2009 are fully consistent with earlier studies, including an increase in ozone density in the upper stratosphere and a decrease below  $\sim 30$  km. They can be understood in terms of meridional circulation cells forced by planetary waves [Garcia, 1987; Randel, 1993, Figure 8]. Planetary wave forcing in the high-latitude winter hemisphere drives a global circulation with a clockwise lower cell ( $< \sim 40$  km) and a counterclockwise upper cell ( $> \sim 40$  km), with both cells

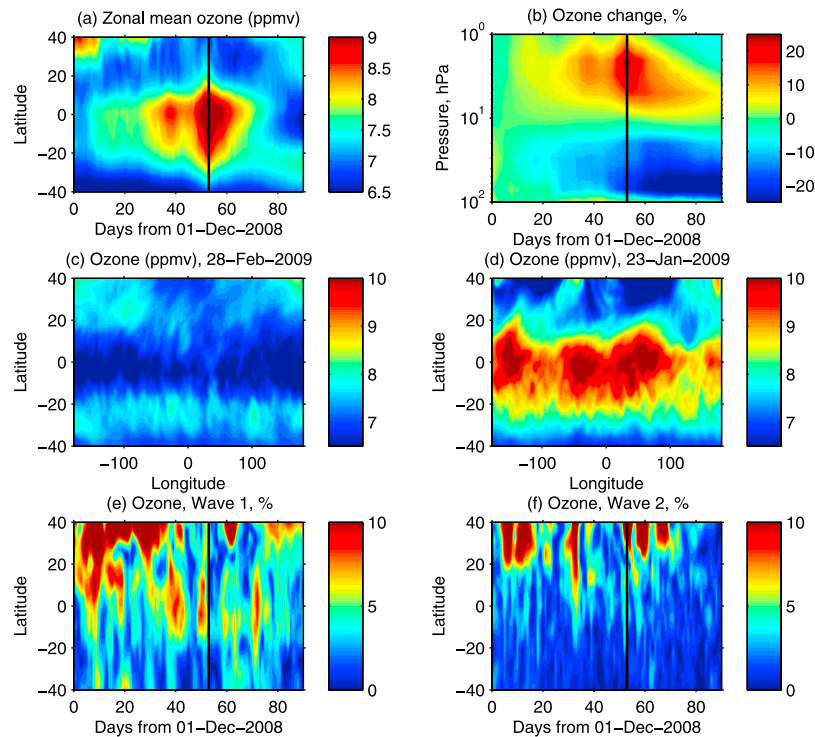


**Figure 2.** (a) Variation in zonal mean ozone mixing ratio at 2 hPa shows distinct increases in ozone mixing ratio coinciding with enhancements in the residual circulation and tropical cooling. (b) Change in ozone as a function of time and pressure, calculated as departure from Dec 1–10 mean. Longitudinal distribution of ozone at 2 hPa (c) during a period of weak planetary waves (Feb 28, 2009) and (d) during the peak of the warming (Jan 23, 2009). (e) Wave 1 and (f) wave 2 in ozone at 2 hPa as a percentage of the zonal mean.

extending well into the summer hemisphere. The adiabatic effects drive a warming in the high-latitude stratosphere and a cooling in the tropical stratosphere. The mesospheric effects have the opposite character, with mesospheric cooling in high latitudes and mesospheric warming in the tropics. Vertical transport associated with these cells is upward in the tropical stratosphere and downward in the tropical mesosphere. Thus, the increase in the low-latitude ozone density between 30–50 km is driven by several mechanisms: 1) upward transport of ozone from the ozone-rich lower stratosphere as indicated by Figure 2b, 2) meridional transport from the Southern to the Northern hemisphere, and 3) longer ozone lifetime in the photochemically controlled upper stratosphere due to the tropical cooling. The increase in ozone density that is shown in Figure 2b is expected to strengthen the amplitude of the migrating semidiurnal tide.

[11] For weak planetary wave conditions the longitudinal distribution of stratospheric ozone is approximately uniform (Figure 2c). This zonally symmetric distribution drives the generation of the migrating semidiurnal tide. When planetary wave forcing generates anomalous circulation cells, the longitudinal distribution of ozone becomes more asymmetric (Figure 2d) and can lead to the generation of a non-migrating semidiurnal tide. Figures 2e and 2f show amplitudes of wave 1 and wave 2 in the ozone mass mixing ratio as functions of time and latitude and indicate that zonal asymmetries in the ozone distribution become stronger after amplifications in the planetary wave activity.

[12] As ionospheric electron density is sensitive to the tidal variations through the E-region dynamo mechanism,

increased variations in tidal modes are expected to generate increased variations in the ionospheric electron density and in TEC. Figure 3 demonstrates diurnal behavior in TEC in the northern crest of the equatorial ionization anomaly (3°N, 75°W) for the period Dec 1, 2008–Mar 1, 2009, with Figure 3a presenting IRI (International Reference Ionosphere) model output and Figure 3b presenting observations of GPS TEC. According to IRI, TEC change during this period is dominated by a seasonal variation, with minimum daytime TEC predicted on January 15. In the second half of February, daytime TEC values start departing from the mean values calculated for the Dec 8–Jan 8 period due to the beginning of the transition to spring season. We note that the mean IRI TEC overestimates GPS TEC by ~30%, likely due to extreme solar minimum, but correctly represents the diurnal behavior in TEC. Another notable feature is a large day-to-day variability in GPS TEC that is not present in the model. To characterize this variability, we compute TEC variances as departure from the mean value during the daytime (9–21 LT), with mean value obtained from Dec 8–Jan 8 data. Figure 4a shows these variances for a range of latitudes in the 75°W longitudinal sector. To minimize effects of the seasonal transition, we limit data presentation to February 18 (day 80). Large variances are typically observed in the northern and southern crests of equatorial ionization anomaly (~3°N and 27°S). Particularly large variances are observed for a prolonged time period (~25 days) after the peak of the SSW and coincide with a change in the stratospheric ozone shown in Figure 2b. The observed ionospheric variability by far exceeds the



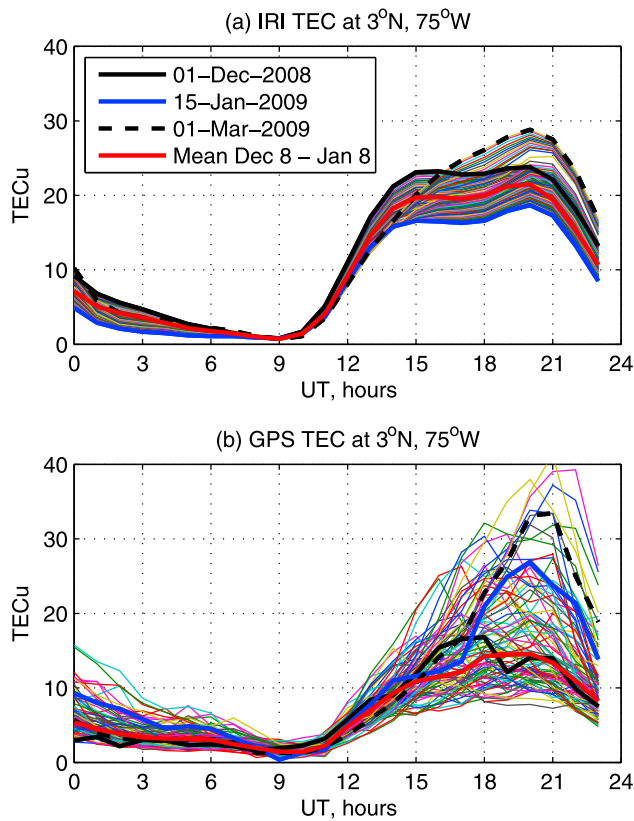


**Figure 3.** Total electron content in the northern crest of the equatorial ionization anomaly ( $3^{\circ}\text{N}$ ,  $75^{\circ}\text{W}$ ) (a) from the IRI model and (b) from the GPS TEC measurements.

variability expected from the IRI model, as shown in Figure 4b. To facilitate comparison, IRI variances (blue line) are multiplied by a factor of 5. The essential feature of the observed ionospheric behavior is large variability that is not

related to the geomagnetic activity (indicated by the Kp index) or seasonal changes (indicated by the IRI model). As it coincides with the ozone increase shown in Figures 2a and 2b, we suggest that the ionosphere responds to the modified tidal forcing.

[13] *Sridharan et al.* [2012] found a sustained increase in the amplitude of the semidiurnal tide in the tropical mesosphere after SSW, and linked it to the increase in the stratospheric ozone. *Pedatella and Forbes* [2010] reported a prolonged increase in the amplitudes of both migrating and non-migrating semidiurnal tides in GPS TEC data during the same time period as ozone density increase and increase in TEC variances shown in this study in Figures 2 and 4. *Goncharenko et al.* [2010b] found that effects of the 2009 SSW could be identified in the low-latitude ionosphere for at least three weeks after the peak in stratospheric temperatures. Analysis of COSMIC data indicated that the ionospheric response to the 2009 SSW lasted for  $\sim 25$  days, with enhanced migrating tides playing a dominant role and non-migrating tides playing a secondary role in ionospheric effects [*Lin et al.*, 2012]. These observations are fully consistent with our report of a sustained increase in the ozone density and an enhanced longitudinal asymmetry in ozone density that should lead to the amplification of both migrating and non-migrating semidiurnal tides and produce ionospheric perturbations.

[14] To summarize, quasi-stationary planetary waves that attain high amplitudes in the wintertime high-latitude stratosphere force large-scale circulation changes that reach the tropical stratosphere. The nature of these circulation changes leads to the long-lasting increase in tropical ozone density around the peak ozone heating rates ( $\sim 30$ – $50$  km), where a migrating semidiurnal tide is generated through the absorption of solar UV. In addition, circulation changes amplify longitudinal inhomogeneities in the ozone distribution that can lead to the generation of the non-migrating tides. Perturbations in the ozone density are strongest during

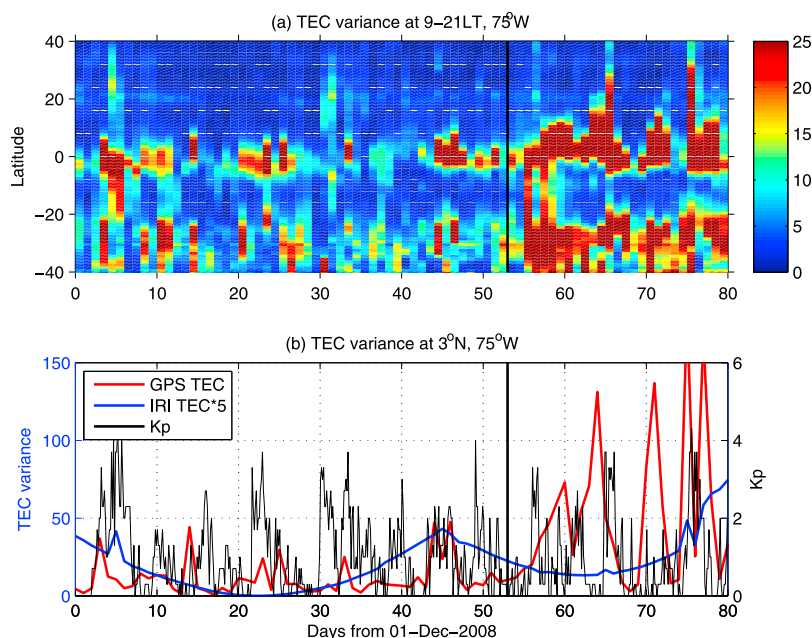


**Figure 4.** (a) GPS TEC variance at  $75^{\circ}\text{W}$ . (b) TEC variance at  $75^{\circ}\text{W}$  and  $3^{\circ}\text{N}$  from GPS TEC observations (red) and from the IRI model (blue). The IRI TEC variance is multiplied by a factor of 5. The black line indicates the Kp index.

the SSW and last for over 35 days. Our results also indicate that high planetary wave activity that does not lead to sudden stratospheric warmings still forces similar variations in the tropical stratospheric ozone, albeit with smaller magnitude and shorter duration. Large and persistent variability in the ionospheric total electron content is observed in the low-latitude ionosphere coinciding with the ozone changes, and long after the decrease in planetary wave activity. We suggest that ozone perturbation is one of the important mechanisms connecting terrestrial and space weather.

[15] **Acknowledgments.** Work at the MIT Haystack Observatory has been supported by NSF Co-operative Agreement ATM-0733510 with the Massachusetts Institute of Technology and by NSF ATM 6920184. Work at the MIT EAPS Department has been supported through NSF grant ATM 0808831. The authors thank the International Space Science Institute (ISSI) for sponsoring the team meetings on this research topic. ECMWF Interim data used in this study have been obtained from the ECMWF Data Server.

[16] The Editor thanks J. Lastovicka and an anonymous reviewer for their assistance in evaluating this paper.

## References

- Andrews, D. G., J. R. Holton, and C. B. Leovy (1987), *Middle Atmosphere Dynamics*, 489 pp., Academic, San Diego, Calif.
- Chau, J. L., B. G. Fejer, and L. P. Goncharenko (2009), Quiet variability of equatorial ExB drifts during a sudden stratospheric warming event, *Geophys. Res. Lett.*, **36**, L05101, doi:10.1029/2008GL036785.
- Dee, D. P., et al. (2011), The ERA-Interim reanalysis: Configuration and performance of the data assimilation system, *Q. J. R. Meteorol. Soc.*, **137**, 553–597, doi:10.1002/qj.828.
- Forbes, J. M., and H. B. Garrett (1978), Thermal excitation of atmospheric tides due to insolation absorption by O<sub>3</sub> and H<sub>2</sub>O, *Geophys. Res. Lett.*, **5**, 1013–1016, doi:10.1029/GL005i012p01013.
- Fritz, S., and S. D. Soules (1970), Large-scale temperature changes in the stratosphere observed from Nimbus III, *J. Atmos. Sci.*, **27**, 1091–1097, doi:10.1175/1520-0469(1970)027<1091:LSTCIT>2.0.CO;2.
- Fuller-Rowell, T., H. Wang, R. Akmaev, F. Wu, T.-W. Fang, M. Iredell, and A. Richmond (2011), Forecasting the dynamic and electrodynamic response to the January 2009 sudden stratospheric warming, *Geophys. Res. Lett.*, **38**, L13102, doi:10.1029/2011GL047732.
- Garcia, R. R. (1987), On the mean meridional circulation of the middle atmosphere, *J. Atmos. Sci.*, **44**, 3599–3609, doi:10.1175/1520-0469(1987)044<3599:OTMMCO>2.0.CO;2.
- Goncharenko, L., and S.-R. Zhang (2008), Ionospheric signatures of sudden stratospheric warming: Ion temperature at middle latitude, *Geophys. Res. Lett.*, **35**, L21103, doi:10.1029/2008GL035684.
- Goncharenko, L. P., J. L. Chau, H.-L. Liu, and A. J. Coster (2010a), Unexpected connections between the stratosphere and ionosphere, *Geophys. Res. Lett.*, **37**, L10101, doi:10.1029/2010GL043125.
- Goncharenko, L. P., A. J. Coster, J. L. Chau, and C. E. Valladares (2010b), Impact of sudden stratospheric warmings on equatorial ionization anomaly, *J. Geophys. Res.*, **115**, A00G07, doi:10.1029/2010JA015400.
- Hagan, M. E., M. D. Burrage, J. M. Forbes, J. Hackney, W. J. Randel, and X. Zhang (1999), GSWM-98: Results for migrating solar tides, *J. Geophys. Res.*, **104**(A4), 6813–6827, doi:10.1029/1998JA900125.
- Limpasuvan, V., D. W. J. Thompson, and D. L. Hartmann (2004), The life cycle of the northern hemisphere sudden stratospheric warmings, *J. Clim.*, **17**, 2584–2596, doi:10.1175/1520-0442(2004)017<2584:TLCOTN>2.0.CO;2.
- Lin, J. T., C. H. Lin, L. C. Chang, H. H. Huang, J. Y. Liu, A. B. Chen, C. H. Chen, and C. H. Liu (2012), Observational evidence of ionospheric migrating tide modification during the 2009 stratospheric sudden warming, *Geophys. Res. Lett.*, **39**, L02101, doi:10.1029/2011GL050248.
- Liu, H.-L., W. Wang, A. D. Richmond, and R. G. Roble (2010), Ionospheric variability due to planetary waves and tides for solar minimum conditions, *J. Geophys. Res.*, **115**, A00G01, doi:10.1029/2009JA015188.
- Liu, H., M. Yamamoto, S. Tulasi Ram, T. Tsugawa, Y. Otsuka, C. Stolle, E. Doornbos, K. Yumoto, and T. Nagatsuma (2011), Equatorial electrodynamics and neutral background in the Asian sector during the 2009 stratospheric sudden warming, *J. Geophys. Res.*, **116**, A08308, doi:10.1029/2011JA016607.
- Pancheva, D., and P. Mukhtarov (2011), Stratospheric warmings: The atmosphere-ionosphere coupling paradigm, *J. Atmos. Sol. Terr. Phys.*, **73**, 1697–1702, doi:10.1016/j.jastp.2011.03.006.
- Pedatella, N. M., and J. M. Forbes (2010), Evidence for stratosphere sudden warming-ionosphere coupling due to vertically propagating tides, *Geophys. Res. Lett.*, **37**, L11104, doi:10.1029/2010GL043560.
- Randel, W. J. (1993), Global variations of zonal mean ozone during stratospheric warming events, *J. Atmos. Sci.*, **50**, 3308–3321, doi:10.1175/1520-0469(1993)050<3308:GVOZMO>2.0.CO;2.
- Rideout, W., and A. Coster (2006), Automated GPS processing for global total electron content data, *GPS Solut.*, **10**, 219–228, doi:10.1007/s10291-006-0029-5.
- Sridharan, S., et al. (2012), Variabilities of mesospheric tides during sudden stratospheric warming events of 2006 and 2009 and their relationship with ozone and water vapour, *J. Atmos. Sol. Terr. Phys.*, **78–79**, 108–115, ISSN 1364–6826, doi:10.1016/j.jastp.2011.03.013.

A. J. Coster and L. P. Goncharenko, Haystack Observatory, Massachusetts Institute of Technology, Rte. 40, Westford, MA 01886, USA. (lpg@haystack.mit.edu)

D. I. V. Domeisen and R. A. Plumb, Department of Earth, Atmospheric and Planetary Sciences, Massachusetts Institute of Technology, 77 Massachusetts Ave., Cambridge, MA 02139, USA.